DENSITY RATIO EFFECTS ON THE COOLING PERFORMANCES OF A COMBUSTOR LINER COOLED BY A COMBINED SLOT/ EFFUSION SYSTEM

Proceedings of ASME Turbo Expo 2012
GT2012
June 11-15, 2012, Copenhagen, Denmark

GT2012-68263

DENSITY RATIO EFFECTS ON THE COOLING PERFORMANCES OF A COMBUSTOR LINER COOLED BY A COMBINED SLOT/ EFFUSION SYSTEM

A. Andreini, G. Caciolli, B. Facchini, L. Tarchi
Energy Engineering Department "Sergio Stecco"
University of Florence
50139, via Santa Marta 3, Florence, Italy
Email: gianluca.caciolli@htc.de.unifi.it
www.htc.de.unifi.it

D. Coutandin, A. Peschiulli, S. Taddei
Engineering, R&D
AVIO S.p.A.
Rivalta (TO) - Italy
Daniele.Coutandin@aviogroup.com

ABSTRACT

The aim of the present study is to investigate the effects of density ratio between coolant and mainflow on a real engine cooling scheme of a combustor liner. Measurements of heat transfer coefficient and adiabatic effectiveness were performed by means of a steady-state Thermochromic Liquid Crystals (TLC) technique; experimental results were used to estimate, through a 1D thermal procedure (Therm1d), the Net Heat Flux Reduction and the overall effectiveness in realistic engine working conditions.

In order to reproduce a representative value of combustor coolant to mainstream density ratio, tests were carried out feeding the cooling system with carbon dioxide (CO_2), while air was used in the main channel; to highlight the effects of density ratio and, as a consequence, to distinguish between the influence of blowing ratio and velocity ratio, tests were replicated using air both as coolant and mainstream and results were compared.

The experimental analysis was performed on a test article replicating a slot injection and an effusion array with a central large dilution hole. Test section consists of a rectangular cross-section duct and a flat perforated plate provided with 272 holes arranged in 29 staggered rows (d=1.65 mm, $\alpha = 30°$, L/d=5.5). Furthermore a dilution hole (D =18.75 mm) is located at the 14^{th} row; both effusion and dilution holes are fed by a channel replicating a combustor annulus. The rig allows to control mainstream and coolant flow parameters, especially in terms of Reynolds number of mainstream and effusion holes. Located upstream the first effusion row, a 6.0 mm high slot ensures the protection of the very first region of the liner.

Experiments were carried out imposing several values of effusion blowing and velocity ratios within a range of typical modern engine working conditions (BR_{eff}/VR_{eff} = 1.5; 3.0; 5.0; 7.0) and keeping constant slot flow parameters ($BR_{sl} \approx 1.5$).

Results point out the influence of density ratio on film cooling performance, suggesting that velocity ratio is the driving parameter for the heat transfer phenomena; concerning the effectiveness, results show that the adiabatic effectiveness is less sensitive to the cooling flow parameters, especially at the higher blowing/velocity ratios.

OVERVIEW

Over the last ten years, the effort to reduce NO_x emissions has been leading the development of aeroengine combustor in order to meet stricter legislation requirements. Some very encouraging results have already been obtained but the achieved solutions have created other technical problems.

To satisfy future ICAO standards concerning NO_x emissions, main engine manufacturers have been updating the design concept of combustors. Future aeroengines combustion devices will operate with very lean mixtures in the primary combustion zone, switching as much as possible to premixed flames. Whatever detailed design will be selected, the amount of air in the primary zone will grows significantly at the expense of liner cooling air, which will be reduced. Consequently, important attention must be paid to the appropriate design of the liner cooling system, in order to optimize coolant consumption and guarantee an effective liner protection. In addition, further goals need to be taken into account: reaction quenching due to a sudden mixing with cooling air should be accurately avoided, whilst temperature distribution has to reach the desired levels in terms of OTDF.

In recent years, the improvement of drilling capability has

allowed to make a large quantity of extremely small cylindrical holes, whose application is commonly referred to as effusion cooling. Alternative solutions to the typical 2D slot combustor cooling systems, like the full coverage film cooling or multihole film cooling, still relies on the generation of a high effectiveness layer of film cooling; on the contrary, an effusion cooling system permits to lower the wall temperature mainly through the so called "heat sink effect", which is the wall cooling due to the heat removed by the passage of the coolant through the holes [1, 2]. A high number of small holes uniformly distributed over the whole surface allows, if accurately designed, a significant improvement in lowering wall temperature, despite a slight reduction of the wall protection at least in the first part of the liner. Even if early effusion cooling schemes were developed to be an approximation of transpiration cooling, it is important to observe that present combustor effusion cooling design is usually based on very shallow injection holes (less than 30°) with high coolant jet momentum. This updated angled effusion cooling allows to greatly increase the heat sink effect (higher holes Reynolds number, and higher exchange areas) without excessive detriment to film effectiveness. With this design approach the analysis and the characterization of the heat transfer and the wall protection due to the injection of coolant becomes a fundamental issue in order to estimate the entire cooling system performance.

Many studies of full coverage film cooling have been focused on measuring or estimating the film effectiveness generated by coolant jets and the heat transfer of effusion cooling. Scrittore et al. [3] studied the effects of dilution hole injection on effusion behaviour; they found relevant turbulence levels downstream dilution holes, thus leading to an increased spreading of coolant jets. Scrittore et al. [4] measured velocity profiles and adiabatic effectiveness of a full coverage scheme with blowing ratios from 3.2 to 5.0, finding the attainment of a fully developed effectiveness region at the 15^{th} row and a very low effect of blowing ratio on cooling performance. Metzger et al. [5] studied the variation of heat transfer coefficient for full-coverage film cooling scheme with normal holes, founding an augmentation of 20-25% in the local heat transfer with blowing ratio 0.1 and 0.2. Crawford et al. [6] experimentally determined Stanton number for an effusion cooling geometry. Martinez-Botas et al. [7] measured heat transfer coefficient and adiabatic effectiveness of a variety of geometries in a flat plate to test the influence of the injection angle varying blowing ratio from 0.33 to 2.0. They measured the variation of the heat transfer coefficient h with respect to a reference case h_0; main result was a maximum of h/h_0 close to the hole and further downstream with highest heat transfer augmentation for 30° injection angle. Kelly and Bogard [8] investigated an array of 90 normal holes finding that the largest values for h/h_0 occur immediately downstream of the film cooling holes and the levels of h/h_0 are similar for the first 9 rows. They explained that this could be due to an increase in the local turbulence levels immediately downstream of the holes, created by the interaction between the cooling jet and the mainstream flow. Another reason could be the creation of a new thermal boundary layer immediately downstream of the cooling jets. In the open literature none of the previous studies investigates the effect that a high blowing ratio has on adiabatic effectiveness, heat transfer coefficient and net heat flux reduction. As reported by Kelly and Bogard [8], increases in heat transfer coefficient due to high blowing ratios could potentially be replaced by an increase in heat transfer coefficient due to high mainstream turbulence. More recently Facchini et al. [9, 10] measured the overall effectiveness and the heat transfer coefficient at variable blowing ratios on a real engine cooling scheme to evaluate the combined effects of slot, effusion and a large dilution hole; they found that an increase in BR leads to lower values of effectiveness. On the other hand, they found that high BR values enhance the heat transfer phenomena. Facchini et al. [11] investigated also the influence of a recirculating area in the mainstream on the same geometry; they highlight that the presence of the recirculation leads to a general reduction of effectiveness, while it does not have significant effects on the heat transfer coefficient.

Despite many studies deal with investigating the effusion cooling performance, most of them were conducted using air as coolant and mainflow, precluding the possibility to point out the effects of density ratio between the two flows. Density ratio is, however, a key parameter for the design of a combustor liner cooling system, mainly because of the actual large temperature difference between coolant and burned gases inside the core. Ekkad et al. [12, 13] measured effectiveness and heat transfer coefficient distribution over a flat surface with one row of injection holes inclined streamwise at 35° for several blowing ratios and compound angles; tests were carried out using air and carbon dioxide as coolant, finding that both heat transfer and effectiveness increase with blowing ratio. They also pointed out the effects of density ratio, showing how these effects are more evident with increasing the compound angle and the momentum flux ratio. This experimental survey was, however, oriented for turbine blade applications rather than combustors. More recently, Lin et al. [14, 15] investigated both experimentally and numerically adiabatic film cooling effectiveness of four different 30° inclined multihole film cooling configurations; the survey, which was specific for combustor liner applications, was performed using a mixture of air and CO_2 as coolant, but it was mainly focused on studying the influence of hole geometrical parameters and blowing ratio on film cooling rather than on the effects of density ratio. Andreini et al. [16] performed a CFD analysis on the a test article replicating a slot injection and an effusion array; they simulated the behavior of the cooling system both with air and CO_2. Numerical results show that the entity of local heat transfer enhancement in the proximity of effusion holes exit is due to gas-jets interaction and that it mainly depends on effusion velocity ratio; furthermore a comparison between results obtained with air and with CO_2 as coolant pointed out the effects of density ratio, showing the opportunity to scale the increase in heat transfer coefficient with effusion jets velocity ratio.

In the present study heat transfer coefficient, adiabatic effectiveness, NHFR and overall effectiveness are investigated on a test rig replicating a real cooling system for a combustor liner application; tests are carried out using air and CO_2 as cooling

flows, in order to point out the effects of density ratio, and imposing real engine values of velocity and blowing ratios.

NOMENCLATURE

A	Reference area	$[m^2]$
BR	Blowing Ratio	$[-]$
Cd	Hole discharge coefficient	$[-]$
d	Effusion hole diameter	$[m]$
D	Dilution hole diameter	$[m]$
DR	Density Ratio	$[-]$
HTC	Heat Transfer Coefficient	$[W/m^2K]$
L	Hole length	$[m]$
Ma	Mach number	$[-]$
m	Mass flow rate	$[kg/s]$
p	Pressure	$[Pa]$
q	Heat flux	$[W/m^2]$
Re	Reynolds number	$[-]$
s	Slot lip thickness	$[m]$
S_x	Streamwise pitch	$[m]$
S_y	Spanwise pitch	$[m]$
T	Temperature	$[K]$
VR	Velocity Ratio	$[-]$
x	Abscissa along the plate	$[m]$
y	Spanwise location	$[m]$

Greeks

α	Effusion hole injection angle	$[deg]$
η	Effectiveness	$[-]$
γ	Ratio of specific heat	$[-]$
θ	Dimensionless temperature	$[-]$
ρ	Density	$[kg/m^3]$

Subscript

aw	Adiabatic wall
c	Coolant
conv	Convection
eff	Effusion
is	Isoentropic
main	Mainstream
ov	Overall
ref, 0	Reference
sl	Slot
T	Total
w	Wall

Acronyms

CO_2	Carbon Dioxide
FEM	Finite Element Method
$ICAO$	International Civil Aviation Organization
$NEWAC$	NEW Aeroengine Core concept
$NHFR$	Net Heat Flux Reduction
$OTDF$	Outlet Temperature Distribution Factor
$PMMA$	Poly-Methyl Methacrylate
PVC	Polyvinyl Chloride
TLC	Thermochromic Liquid Crystal

EXPERIMENTAL APPARATUS

This investigation was aimed at pointing out the dependence of film cooling performance from coolant-to-mainstream density ratio. In order to achieve this goal, measurements on a test rig representing a specific cooled combustor liner were carried out using air and carbon dioxide (CO_2) as cooling flows and results were compared in term of adiabatic effectiveness, heat transfer coefficient, Neat Heat Flux Reduction (NHFR) and overall effectiveness.

The test rig, depicted in Figure 1, consists of an open-loop suction type wind tunnel which allows the complete control of three separate flows: the hot mainstream, the slot cooling and the effusion cooling flows. The vacuum system is made up of two rotary vane vacuum pumps with a capacity of 900 m^3/h each dedicated to the extraction of the mainstream mass flow.

The mainstream flow rate is set up by guiding the speed of the pumps and using a calibrated orifice located at the beginning of the wind tunnel (throttle). The mainstream temperature is set up using a 24.0 kW electronically controlled electric heater, placed at the inlet of the rig.

Slot and effusion coolant flows reach the test rig crossing two different lines that connect the wind tunnel with a pressure tank which stores the cooling fluid up to a maximum pressure of 1 MPa. Flow rates are set up by throttling two separated valves. Heaters for a total power of 1.5 kW are placed along the lines which connect the tank to the rig, in order to set the desired inlet coolant temperature.

The mass flow rate is measured in three different locations of the rig: according to the standard EN ISO 5167-1 one orifice measures the flow rate blown by the pumps, while two orifices measure the slot and the effusion mass flow rates.

Two pressure scanners Scanivalve DSA 3217 with temperature compensated piezoresistive relative pressure sensors measure the static pressure in 32 different locations with a maximum accuracy of 6.9 Pa. Several T type thermocouples connected to a data acquisition/switch unit (HP/Agilent® 34970A) measure the mainstream and the coolant static temperatures.

The main channel has a constant cross section of 100x150 mm and is 1000 mm long. In the first part of the channel the mainstream flow crosses a honeycomb and three screens which allow to set an uniform velocity profile. A 6.0 mm square hole grid (hole pitch 7.6 mm, plate thickness 0.7 mm) is placed 125 mm upstream the slot coolant injection, so as to set turbulence level at x/S_x=0 around 5%, with a macroscopic length scale of 2.8 mm, according to correlations proposed by Roach [17].

Heat transfer coefficient and effectiveness are determined by a steady state technique, measuring wall temperatures from a heated surface, using TLC paint. Wide band TLC 30C20W supplied by Hallcrest and active from $\sim 30^\circ C$ to $50^\circ C$ are used. Crystals are thinned with water and sprayed with an airbrush on the test surface after the application of a black background paint. TLC were previously calibrated following the steady state gradient method (Chen et al. [18]). The calibration setup is made by a 4.5 mm thin aluminium rectangular plate, housing seven thermocouples, sprayed with black background paint and then TLC.

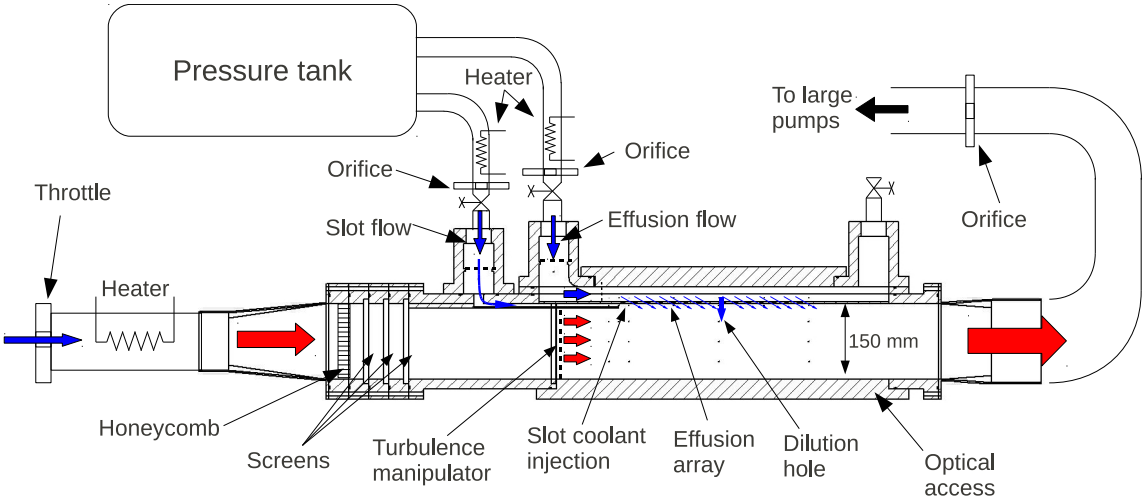

FIGURE 1. Sketch of the test rig.

One of its edges is heated by an electric heater, while the other is cooled by air. The whole apparatus is housed into an insulating basis. Camcorder and illuminating system are placed at the same distance and inclination of the real test, so as to replicate the exactly alike optic conditions. A linear temperature gradient will appear on TLC surface: once steady conditions are reached, a single picture is sufficient for a precise measurement of color-temperature response, with the latter parameter measured through thermocouples. Several tests have been carried out, so as to increase global precision; moreover the calibration has been checked directly on the test article before each experiment.

A digital camera (Sony XCD-SX90CR) records color bitmap images (1280x960*pixel*) from the TLC painted surface on a PC. The illuminating system (Shott-Fostec KL1500 LCD) uses an optical fiber goose-neck to ensure a uniform illumination on the test surface and it allows to keep both color temperature and light power constant. The test article is completely made of transparent PMMA, thus allowing the required optical access for TLC measurements; the effusion plate only was made of PVC.

Geometry

Figure 2 reports a sketch of the test article, which represents the cooling system of the combustor prototype developed within the European Integrated Project NEWAC. A picture of the prototype is shown in Figure 3. The slot coolant representing the starter film cooling is injected in the mainstream from a 6.0 *mm* high channel, with a lip thickness of 3.0 *mm*. The effusion array and the dilution hole are fed by an annulus with a rectangular 30.0 *mm* high and 120.0 *mm* wide cross-section.

The effusion geometry consists of a staggered array of 272 circular holes (d=1.65 *mm*), with an inclination angle of $\alpha = 30°$, drilled in a 4.5 *mm* thick PVC plate and with a length to diameter ratio of $L/D = 5.5$. The spanwise and the streamwise pitches are respectively S_y=9.9 *mm* and S_x=12.6 *mm*. The first row is located 22.25 *mm* (1.77S_x) after the slot injection, while the last row 375 *mm* downstream. The origin of the coordinate system (x=0)

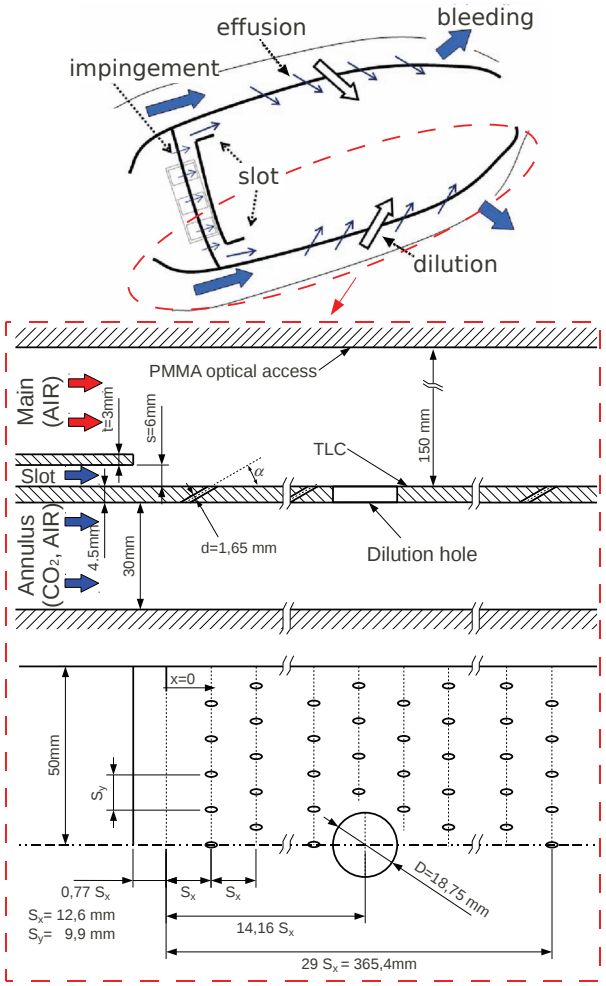

FIGURE 2. Liner geometry.

was set in order to have $x/S_x = 1$ at the first row and $x/S_x = 29$ at the last row, while the slot injection is located at x/S_x=-0.77. The dilution hole (D=18.75 *mm*) is located immediately after the 14^{th} row, at x/S_x=14.16.

FIGURE 3. Combustor prototype of European Project NEWAC.

Flow Type (Coolant / Mainstream)	BR_{eff} (VR_{eff})	VR_{eff} (BR_{eff})
AIR / AIR	1.5 (1.5)	-
	3.0 (3.0)	-
	5.0 (5.0)	-
	7.0 (7.0)	-
CO_2 / AIR	1.5 (0.9)	1.5 (2.6)
	3.0 (1.8)	3.0 (5.1)
	5.0 (2.9)	5.0 (8.5)
	7.0 (4.1)	7 (11.9)

TABLE 1. Test matrix.

MEASUREMENTS AND TEST CONDITIONS

The experimental survey was formed by two main campaigns: the first campaign was aimed at measuring the heat transfer coefficient over the effusion plate, which was tested imposing values of blowing ratio and velocity ratio within a typical range of an aeroengine combustor. Afterwards the same fluid conditions were replicated in the second campaign in order to estimate the adiabatic effectiveness of the film cooling generated by the system. Results of the two campaigns were finally combined to calculate the Net Heat Flux Reduction and the overall effectiveness.

In modern combustor the temperature differences between the cooling air and the hot gases lead to a coolant to mainstream density ratio which usually falls within the range 1.5-3.0. In order to reproduce the effects of *DR*, measurements were carried out feeding the cooling system with carbon dioxide (CO_2): including the typical temperature differences required to perform experiments with TLC paint, the use of this foreign gas leads to a $DR \approx 1.7$.

To highlight the effects of density ratio, the test matrix was duplicated and each fluid dynamic condition of the campaign was tested twice: the cooling system was first fed with air and then with CO_2, while hot air was used for the mainflow. Main investigation parameters are defined as follows:

$$BR_{eff} = \frac{1}{N_{row}} \cdot \sum_{k=1}^{N_{row}} BR_k \tag{1}$$

$$BR_k = \frac{Cd_k \cdot (m_{is,k}/\pi d^2/4)}{m_{main,k}/A_{main}} \tag{2}$$

$$VR_{eff} = BR_{eff} \cdot \frac{\rho_{main}}{\rho_{cool}} = \frac{BR_{eff}}{DR} \tag{3}$$

BR_{eff} is the averaged blowing ratio of the effusion rows (the dilution hole was excluded). BR of the k^{th} row was evaluated using the actual mass flow rate through the holes and the correspondent mainstream mass flow (inlet mainstream mass flow and coolant mass flow injected by the previous $(k-1)^{th}$ rows); the amount of coolant crossing each effusion row was calculated using hole discharge coefficient, which is:

$$Cd = \frac{m_{real}}{m_{is}} = \frac{m_{real}}{p_{Tc}\left(\frac{p_{main}}{p_{Tc}}\right)^{\frac{\gamma+1}{2\gamma}} \sqrt{\frac{2\gamma}{(\gamma-1)RT_{Tc}}\left(\left(\frac{p_{Tc}}{p_{main}}\right)^{\frac{\gamma-1}{\gamma}} - 1\right)} \frac{\pi}{4} d^2} \tag{4}$$

It was estimated that $Cd \approx 0.73$. Other parameters are:

$$BR_{sl} = \frac{m_{sl}/A_{sl}}{m_{main}/A_{main}} \tag{5}$$

$$BR_{dil} = \frac{Cd_{dil} \cdot (m_{is,dil}/\pi D^2/4)}{m_{main,14}/A_{main}} \tag{6}$$

A_{main} is the mainstream channel cross-section (150x100 mm^2); A_{sl} is the slot cross section (6x100 mm^2); $Cd_{dil} \approx 0.6$. When air is used both as cooling and mainstream flows, the temperature differences of the experiments cannot raise the density ratio over $DR \approx 1.1$ and, as a consequence, tests carried out imposing the desired values of VR coincide with tests with the correspondent values of BR imposed.

For a better comprehension of slot and effusion influence on the cooling performance, some tests were performed activating only the effusion cooling flow; when the two cooling systems were tested together, the slot flow was set in order to keep a constant value of $BR_{sl} \approx 1.5$. Mainstream absolute pressure was kept constant at about $p_{main} = 50000\ Pa$ ($Re_{main} \approx 75000$, $Ma_{main} \approx 0.04 - 0.05$), while coolant pressure was varied in order to ensure the desired values of coolant velocity inside the holes.

Table 1 sums up the effusion hole testing conditions of the campaign. The effusion plate was first tested using air as coolant, and then using CO_2; 4 different BR_{eff} and 4 different VR_{eff} were investigated. The full test matrix was made up of 48 experiments:

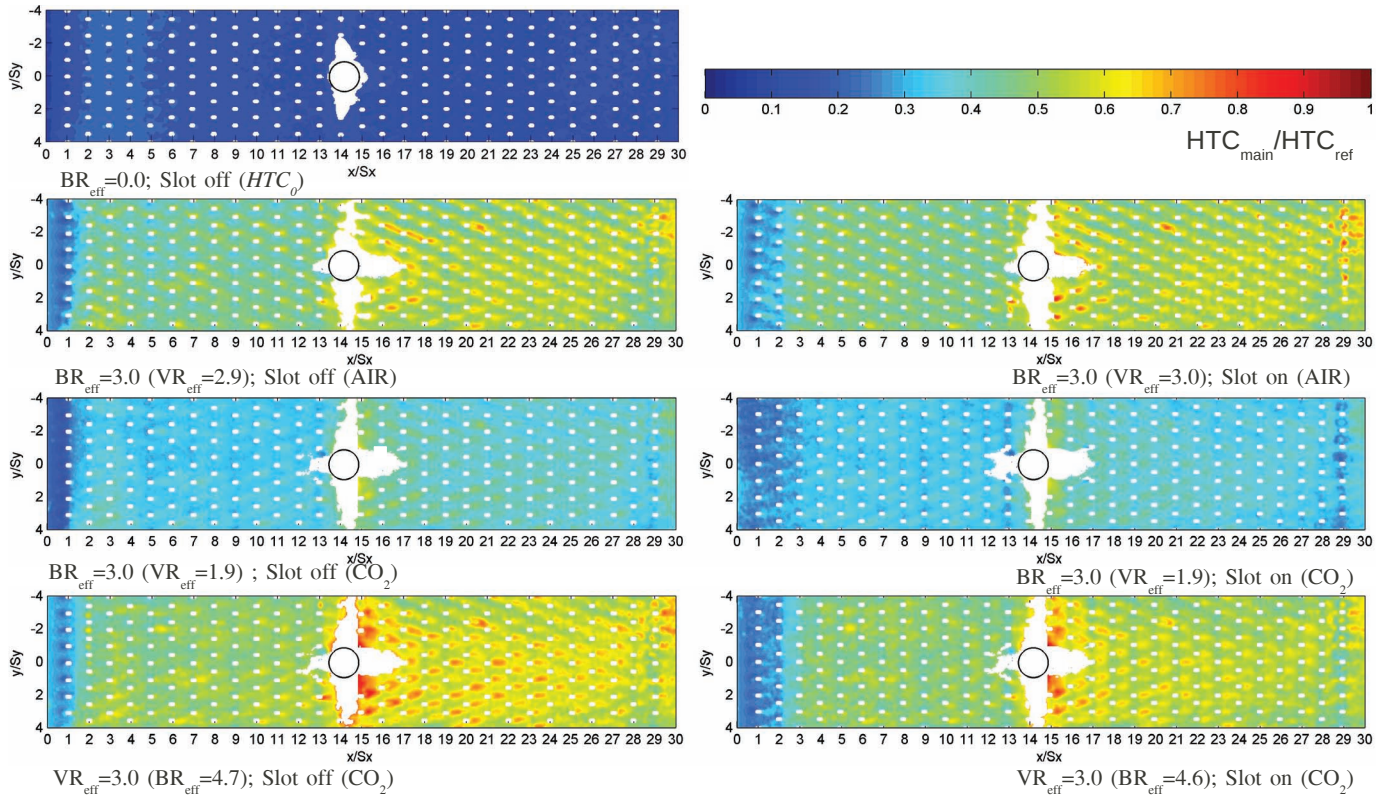

FIGURE 4. Heat transfer coefficients maps ($BR_{eff} - VR_{eff} = 3$).

each point of table 1 was tested twice, feeding or not feeding the slot cooling system (8 AIR/AIR and 16 AIR/CO_2 experiments). The resulting 24 experiments matrix was finally performed twice in order to measure HTC and adiabatic effectiveness. It is important to underline that, in reference to the classification introduced by L'Ecuyer et al. [19], the effusion jets work within the penetration regime ($VR_{eff} > 0.8$) in all testing conditions.

All the tests were run after steady conditions were reached by all the measured quantities: flow rates, pressures and temperatures. The uncertainty analysis was performed following the standard ANSI/ASME PTC 19.1 [20] based on the Kline and Mc-Clintock method [21]. Temperature accuracy is ± 0.5 K, differential pressure ± 6.9 Pa, mass flow rate $\pm 3 - 5\%$; the estimated error for the heat transfer coefficient calculation is $\pm 10\%$, while it is ± 0.05 for the adiabatic effectiveness.

DATA POST PROCESS

Heat transfer measurements

Heat transfer coefficients were determined by a steady state technique, using TLC paint to measure the wall temperature from a heated surface. A heating element, made by a 25.4 μm thick Inconel Alloy 600 foil, has been laser drilled with the same array pitches of the PVC plate, and then applied on the test plate with a double sided tape; surface heat flux is generated by Joule effect, fed by a DC power supply (Agilent® N5763A) which is connected to the Inconel sheet through two copper bus bars fixed on lateral extremities of the test plate.

The mainstream heat transfer coefficient is defined as:

$$HTC_{main} = \frac{q_{conv}}{T_w - T_{main}} \tag{7}$$

where T_{main} is the mainstream static temperature, measured by means of three thermocouple located one pitch upstream the slot injection. T_w is the wall temperature measured by means of TLC while q_{conv} represents the heat rate exchanged by convection between the effusion plate and the mainstream flow. Due to the presence of the effusion and dilution holes, heat generated by the Inconel foil is not uniform on the surface of the plate; in addiction, test sample is not ideally adiabatic and heat losses due to the conduction through the plate and the convective heat removed by coolant both in the annulus and inside the holes have to be taken into account. As a consequence, in order to have an accurate evaluation of the net heat flux transferred from the surface to the mainstream, q_{conv} was estimated implementing an iterative procedure based on a complete 3D thermal-electric FEM simulation. The procedure evaluates the non uniform heat locally generated on the surface, allowing to obtain an accurate estimate of q_{conv}. Moreover, heat losses are taken into account too: depending on the fluid dynamics conditions of the tests, they are approximately 2% - 5%. A detailed description of the iterative procedure can be found in Facchini et al. [10].

Heat transfer experiments were carried out with coolant and mainstream at room temperature. Likewise effectiveness measurements, the mainstream absolute pressure was kept constant

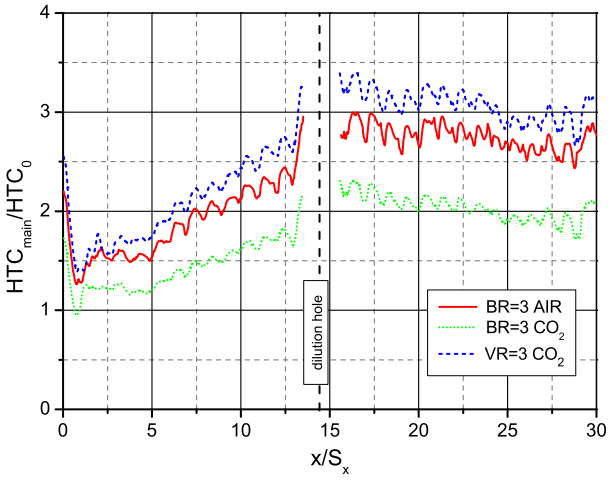

(a) Effusion

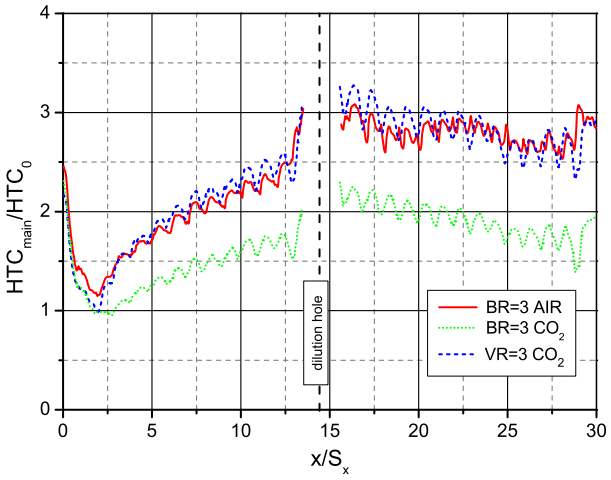

(b) Effusion + Slot

FIGURE 5. Spanwise averaged HTC ($BR_{eff} - VR_{eff} = 3$).

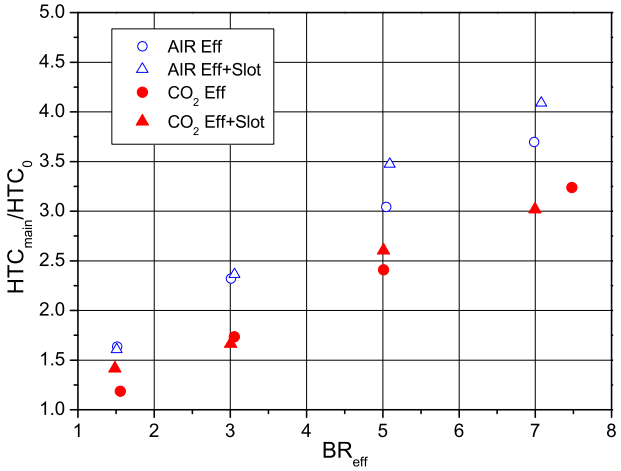

(a) Averaged value of HTC/HTC$_0$ *vs* BR$_{eff}$.

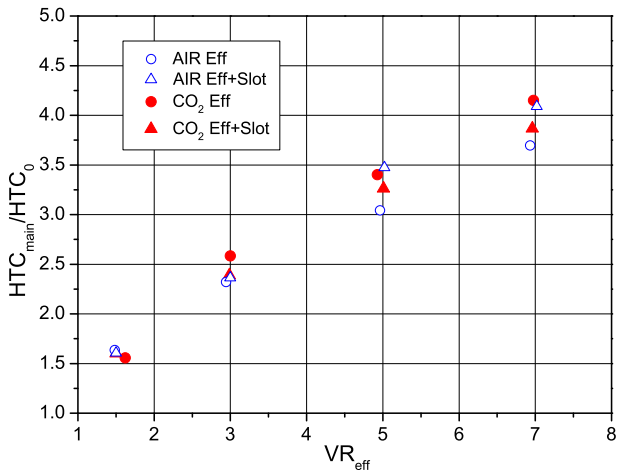

(b) Averaged value of HTC/HTC$_0$ *vs* VR$_{eff}$.

FIGURE 6. Heat transfer coefficient results.

at about p_{main}=50000 Pa, while coolant pressure was varied in order to ensure the desired values of BR_{eff} and VR_{eff}.

Effectiveness measurements

Effectiveness measurements were carried out heating both the coolant and the mainflow, in order to obtain temperature of about 300 K and 350 K respectively. Likewise HTC measurements, the mainstream absolute pressure was kept constant at about p_{main}=50000 Pa, while coolant pressure was varied in order to ensure the desired values of coolant velocity.

Adiabatic effectiveness is defined as:

$$\eta_{aw} = \frac{T_{main} - T_{aw}}{T_{main} - T_{cool}} \tag{8}$$

Three thermocouples located one pitch upstream the slot injection acquired mainstream static temperature T_{main}. Three additional probes were dedicated to measure coolant flow static temperature and were inserted into the annulus, at $x/S_x = 0; 14; 29$; one further probe was located inside the slot channel at $x/S_x = -1$. T_{aw} was evaluated through a post-processing procedure which takes into account the thermal fluxes across the plate due to conduction and due to the coolant inside the annulus and the holes. This procedure is based on a 1D approach and considers the following equation:

$$T_{aw} = T_w - \frac{q}{HTC_{main}} \tag{9}$$

where T_w is the wall temperature measured with TLC. Heat flux across the plate (q) is evaluated through TLC wall temperature, coolant temperature and using the Colburn correlation $Nu = 0.023 Re^{0.8} Pr^{1/3}$ to estimate heat transfer coefficients inside the holes and on the annulus side of the plate; Reynolds and Nusselt numbers were evaluated with the hole diameter and with the annulus cross section hydraulic diameter respectively. Values of HTC_{main} were directly taken from results of the dedicated campaign. Conduction through the PVC was taken into account too.

RESULTS

Heat transfer coefficient

Figure 4 shows heat transfer coefficient maps for the experiments carried out imposing $BR_{eff} - VR_{eff}$=3 (due to the

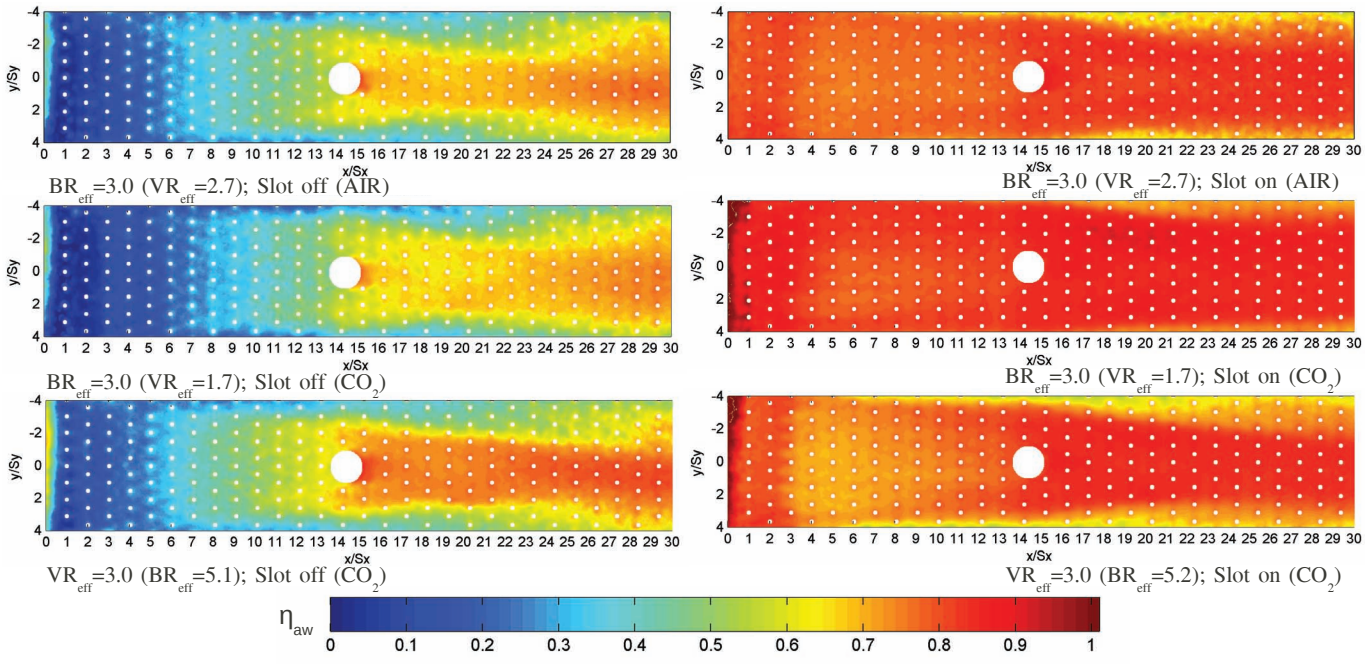

FIGURE 7. Adiabatic effectiveness maps ($BR_{eff} - VR_{eff} = 3$).

small coolant to mainstream density ratio, $VR_{eff} \approx BR_{eff}$ in AIR tests); results are displayed dividing the local HTC_{main} by a constant reference value (HTC_{ref}). In white areas close to the dilution hole HTC was not measured because the local low/high surface heat generation did not allow TLC paints working properly within their activation range. Maps displays the overall trend of HTC, showing that it increases up to the 14^{th} row and then remains nearly constant. Difference between tests with and without slot are restricted to the first 2-3 rows, where coolant coming out from the slot mitigates the heat transfer; after the 5^{th} row, the presence of the slot flow does not alter significantly the behaviour of the effusion cooling.

Imposing the same mainstream conditions of all the other experiments, a reference test was carried out in order to evaluate the heat transfer coefficient without film cooling (HTC_0); map of HTC_0 is displayed in figure 4. Figures 5a and 5b show trends of spanwise averaged heat transfer coefficient along the plate with effusion coolant only and with both slot and effusion flows for $BR_{eff} - VR_{eff}$=3; data are plotted in term of (HTC_{main}/HTC_0) in order to highlight the increase of heat transfer due to coolant injections. Figure 5a shows that HTC remains constant in the first five rows, even if it is enhanced compared to the reference case ($HTC_{main}/HTC_0 > 1$); after the 5^{th} row, it increases up to the dilution hole, where it reaches an asymptotic value. The beginning of the rising trend of HTC is brought forward to the 2-3^{th} row in presence of the slot cooling flow (Figure 5b); however, after the 5^{th} row, the slot flow has only a slight influence on the heat transfer. Results shows that for a constant blowing ratio, heat transfer decreases with increasing the density ratio. Maps and trends are here shown only for one point of the test matrix, which significantly represents the typical behaviour of the system in each testing condition. A more detailed description of the behaviour of heat transfer coefficient over this effusion plate can be found in Facchini et al. [10]. Results of the full test matrix are summarized in Figure 6: it shows the average value of HTC_{main}/HTC_0 of the whole plate with and without the slot flow, plotted versus the actual BR_{eff} (6a) and VR_{eff}(6b). Figures clearly display how the HTC linearly increases with increasing *BR-VR*; furthermore, it is possible to highlight that air tests are in good agreement with CO_2 tests with the same velocity ratio. This means that, within the effusion jets penetration regime, VR acts as the driving parameter of the phenomena instead of BR; this confirms results numerically found by Andreini et al. [16].

Adiabatic effectiveness

Figure 7 shows the adiabatic effectiveness maps for $BR_{eff} - VR_{eff}$ = 3 test points. Maps display the effects of effusion and slot coolant injections and highlight both how the wake generated by the dilution hole and the presence of the slot flow influence the film cooling distribution over the surface. Results point out that, without the slot flow, the effusion system does not guarantee a sufficient protection of the first part of the liner by itself. On the other hand, maps with both effusion and slot coolant show that a very efficient protection of the liner can be obtained combining the two cooling systems. It is also possible to observe that the effusion jets of the first rows destroy the high effectiveness film cooling generated by the slot, leading to a lower η_{aw} area which starts from the 3^{th} row and roughly lasts until the dilution hole.

Figure 8 shows trends of spanwise averaged adiabatic effectiveness along the plate: it is possible to observe that, when only effusion is activated, the film cooling superposition increases η_{aw}

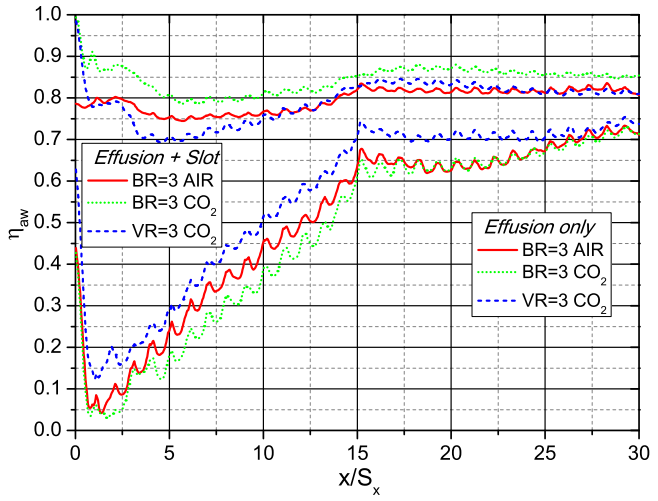

FIGURE 8. Spanwise averaged η_{aw} ($BR_{eff} - VR_{eff} = 3$).

quite linearly until the 15^{th} row, where the dilution hole is located. In the following rows the effectiveness slightly decreases due to the wake of the dilution jet, and finally reaches an asymptotic value at the end of the plate. The presence of the slot coolant strongly enhances the adiabatic effectiveness: according to Andreini et al. [9], after the first three rows, where the η_{aw} remains nearly constant, there is a lower effectiveness area due to the interaction of the slot coolant and the effusion jets; after the dilution hole, η_{aw} reaches an asymptotic value.

Finally Figure 9 shows the averaged adiabatic effectiveness results for the whole test matrix, plotted versus BR_{eff} and VR_{eff}. Tests without slot flow (circles) point out that after $BR_{eff} - VR_{eff} = 3$ adiabatic effectiveness reaches an asymptote and it is weakly affected by these parameters. Even if the penetration of effusion jets increases, and, as a consequence, the effectiveness should decreases, η_{aw} does not fall because the large amount of coolant mass flow injected in the mainstream grows row by row and thus guarantees a good protection of the liner. Experimental results show that within the penetration regime, the effects of coolant to mainstream density ratio are not significant; thus, as commonly found in the literature, BR have to be used to scale the effects of DR.

Concerning tests with both cooling system activated (triangles), results indicate that η_{aw} decreases with increasing BR-VR (due to the increasing penetration of effusion jets), but only slight differences were found changing the coolant to mainstream density ratio. Focusing on tests with the same BR_{eff} (9a), it it is possible to note that an increase in DR cause a small enhancement in η_{aw}; on the other hand, results indicates that, when the both the slot flow and the effusion jets work within the penetration regime, VR_{eff} has to be used to take into account the effects of density ratio.

Net Heat Flux Reduction

Net Heat Flux Reduction (NHFR) is a commonly used parameter to evaluate the reduction of heat flux across a cooled

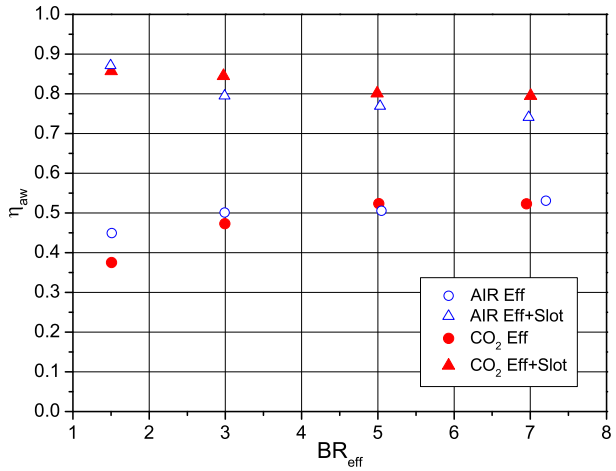

(a) Averaged value of η_{aw} *vs* BR_{eff}.

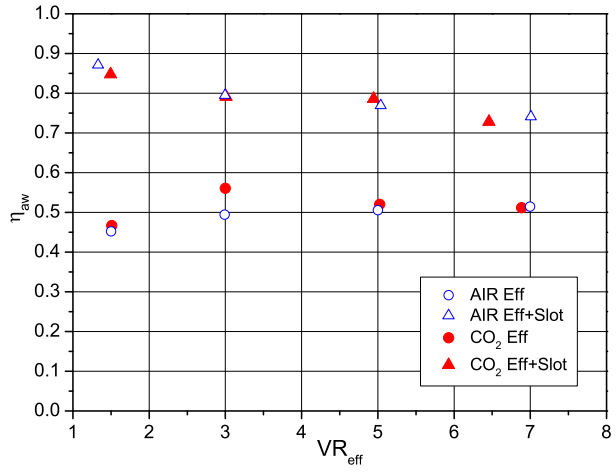

(b) Averaged value of η_{aw} *vs* VR_{eff}.

FIGURE 9. Adiabatic effectiveness results.

surface. This parameter was defined by Sen et al. [22] as:

$$NHFR = 1 - \frac{q}{q_0} = 1 - \frac{HTC_{main}}{HTC_0}(1 - \eta\theta) \qquad (10)$$

where θ represent the dimensionless temperature:

$$\theta = \frac{T_{main} - T_{cool}}{T_{main} - T_w} \qquad (11)$$

In open literature [22,23,24,25] NHFR was mainly used to evaluate turbine endwall and blades cooling systems and the dimensionless temperature was set within the range of $\theta = 1.5 - 1.6$. More recently Facchini et al. [10,11] evaluated NHFR imposing $\theta = 1.2$, a value which is more representative of a combustor. In the present study NHFR was evaluated using the experimental results within a one dimensional thermal procedure (*Therm1d*) in order to estimate an engine representative distribution of θ, taking into account the heating of the coolant inside the effusion holes and hence of the heat sink effect. *Therm1d* is an in-house

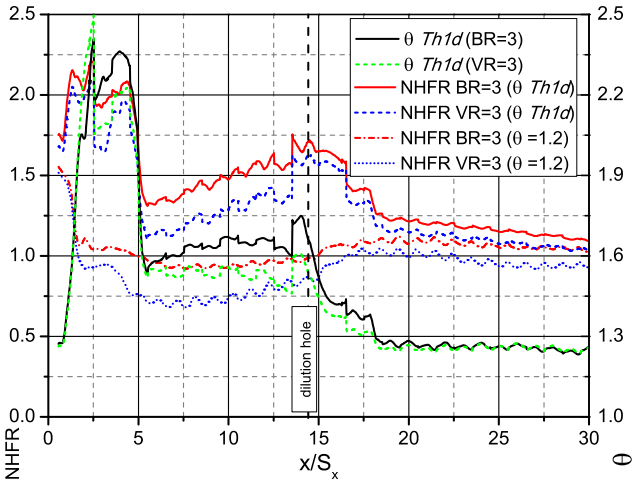

(a) Trends of θ and NHFR ($VR_{eff} - BR_{eff} = 3$).

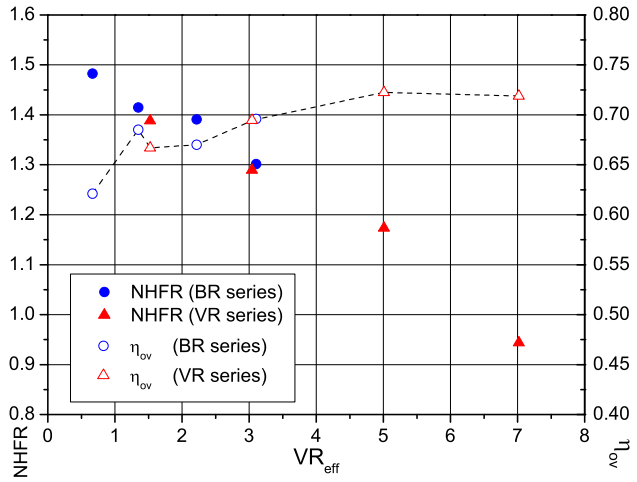

(b) Averaged value of NHFR and η_{ov} *vs* VR_{eff}.

FIGURE 10. Net Heat Flux Reduction and η_{ov} results.

procedure which solves heat conduction inside a combustor liner and provide its temperature distribution using a 1D Finite Difference Model. On the coolant side, the procedure solve the coolant fluid network of the system, taking into account the different cooling techniques of the specific combustor architecture and the heat exchange with metal surfaces; on the hot gas side it estimates the convective heat load and the luminous and the non-luminous radiation through a correlative approach, mainly following the one dimensional approach suggested by Lefebvre [26]. The final temperature distribution is obtained considering also the film cooling and the heat sink effect due to the presence of cooling holes. Further details on the procedure can be found in Andreini et al. [27, 28].

Therm1d was used to set up the cooling fluid network of the test rig, including both the slot and the effusion system; test plate material was specified to be the real steel of NEWAC combustor prototype instead of PVC as in the experiments to more realistically model the conduction through the plate itself. Hot gas boundary conditions were imposed in order to simulate the behaviour of a realistic combustor diffusion flame [27]. Coolant side inlet pressure was varied in order to set the desired averaged BR-VR through the effusion holes and reproduce the experimental test matrix, while inlet coolant temperature and outlet pressure were kept constant. Experimental film cooling and convective gas side HTC distributions were imposed: in order to take into account the effects of density ratio due to the temperature difference between coolant and mainstream, data were taken only from CO_2 tests (only tests with both effusion and slot cooling system). Besides the wall temperature distributions (T_w), each run provided also the local temperature of the coolant coming out from each effusion row (T_{cool}), taking into account its heating through the hole due to the heat removal by heat sink effect. Trends of the θ parameter are shown in Figure 10a for cases $BR_{eff} - VR_{eff}$=3. It is possible to observe how θ varies along the liner as a consequence of a non uniform mainstream temperature distribution and of the resulting T_{cool} and T_w.

Figure 10a displays also trends of NHFR for these two test points: results evaluated through *Therm1d* are compared with those estimated imposing $\theta = 1.2$. As a consequence of the θ behaviour, NHFR calculated considering the heat sink effect is much higher than the simple $\theta-$imposed case (the averaged value is 30% higher for BR case, 70% higher for VR case). Obviously trends evaluated with *Therm1d* are highly affected by the hot gases imposed boundary conditions (e.g. the sharp drop of the 5^{th} row is due to the quick gas temperature rise which represents the flame front), but what is important to highlight is the strong influence of effusion velocity ratio on NHFR. Figure 10b clearly points out how NHFR linearly decreases with VR_{eff}, showing that the opposite effects of rising the effusion velocity ratio (η_{aw} reduction, HTC increase) are detrimental for NHFR.

NHFR results indicate that this cooling configuration always brings to a reduction of the heating flux towards the liner (NHFR>0); nevertheless, this parameter is not properly representative for an effusion cooling system since it does not explicitly take into account the heat sink effect, which instead plays a major role in this type of cooling technique. Furthermore, NHFR cannot reproduce the trade-off shown by this cooling system, that is the growth/decrease of HTC/η_{aw} with increasing VR_{eff}: because of the monotonous drop of this parameter, NHFR cannot be used as a significant design parameter. Therefore, wall temperatures estimated through *Therm1d* were used to calculate also the overall effectiveness of the test plate in real engine conditions. This parameter is defined as:

$$\eta_{ov} = \frac{T_{main} - T_w}{T_{main} - T_{cool}} \tag{12}$$

Results, shown in Figure 10b, highlight that η_{ov} grows up to a maximum for $VR_{eff} = 5$: because of $T_w > T_{cool}$, an increase in HTC_{main} favours the cooling the liner, although the adiabatic effectiveness decreases. Rising VR beyond the peak value is detrimental for the efficiency of the cooling system because the increase of HTC_{main} cannot balance the drop of η_{aw} any further.

CONCLUSION

An experimental and numerical investigation on a real combustor liner cooling system was performed. The cooling scheme consists of a slot injection, followed by a flat plate with 29 effusion rows ($\alpha = 30°$) and a single large dilution hole. The aim of the survey was the investigation of the influence of coolant to mainstream density ratio on the cooling system performances. Values of effusion blowing ratio and velocity ratio typical of modern engine working conditions ($BR_{eff} - VR_{eff}$ =1.5; 3.0; 5.0; 7.0) were imposed in order to measure the heat transfer coefficient and the adiabatic effectiveness; tests were carried out using a steady state technique with wide band thermo-chromic liquid crystals. The effects of density ratio were investigated comparing results obtained feeding the cooling system with both air and CO_2.

HTC results shows that, for a constant blowing ratio, heat transfer is reduced with increasing the density ratio; on the other hand, within the effusion jets penetration regime, velocity ratio is the driving parameter of the phenomena in order to scale the effects of DR. Moving on to the adiabatic effectiveness, experiments show that after $VR_{eff} = 3$, η_{aw} generated by the effusion jets is weakly affected by BR-VR; furthermore, effects of density ratio can be neglected within the penetration regime. When both slot and effusion system are activated, results point out that, for a constant velocity ratio, effectiveness increases with increasing density ratio and that VR_{eff} can be used to take into account the effects of DR. Finally, NHFR and the overall effectiveness were estimated combining heat transfer and effectiveness results: real engine working conditions were simulated using an in-house 1D thermal procedure (*Therm1d*). Results point out a linear decrease of NHFR with VR_{eff}, while η_{ov} shows a maximum, which gives indications about the best working conditions for the cooling system.

ACKNOWLEDGMENT

The authors wish to express their gratitude to Mr. F. Simonetti and Mr. A. Picchi for their useful suggestions and support. The present work was supported by the European Commission as part of FP6 IP NEWAC (NEW Aero engine Core concepts) research program (FP6-030876), which is gratefully acknowledged together with consortium partners.

REFERENCES

[1] Andrews, G. E., Bazdidi-Tehrani, F., Hussain, C. I., and Pearson, J. P., 1991. "Small diameter film cooling hole heat transfer: The influence of hole length". *ASME Paper*(91-GT-344).

[2] Andrews, G. E., Khalifa, I. M., Asere, A. A., and Bazdidi-Tehrani, F., 1995. "Full coverage effusion film cooling with inclined holes". *ASME Paper*(95-GT-274).

[3] Scrittore, J. J., Thole, K. A., and Burd, S. W., 2005. "Experimental characterization of film-cooling effectiveness near combustor dilution holes". *ASME Turbo Expo*(GT2005-68704).

[4] Scrittore, J. J., Thole, K. A., and Burd, S. W., 2006. "Investigation of velocity profiles for effusion cooling of a combustor liner". *ASME Turbo Expo*(GT2006-90532).

[5] Metzger, D., Takeuchi, D., and Kuenstler, P., 1973. "Effectiveness and heat transfer with full-coverage film cooling". *ASME Journal of Engineering for Power,* **95**, pp. 180–184.

[6] Crawford, M. E., Kays, W. M., and Moffat, R. J., 1980. "Full-coverage film cooling - part 1". *Journal of Engineering for Power,* **102**.

[7] Martinez-Botas, R. F., and Yuen, C. H. N., 2000. "Measurement of local heat transfer coefficient and film cooling effectiveness through discrete holes". *ASME Turbo Expo*(2000-GT-243).

[8] Kelly, G. B., and Bogard, D. G., 2003. "An investigation of the heat transfer for full coverage film cooling". *ASME Turbo Expo*(GT2003-38716).

[9] Ceccherini, A., Facchini, B., Tarchi, L., and Toni, L., 2009. "Combined effect of slot injection, effusion array and dilution hole on the cooling performance of a real combustor liner". *ASME Turbo Expo*(GT2009-60047).

[10] Facchini, B., Maiuolo, F., Tarchi, L., and Coutadin, D., 2010. "Combined effect of slot injection, effusion array and dilution hole on the heat transfer coefficient of a real combustor liner - part 1 experimental analysis". *ASME Turbo Expo*(GT2010-22936).

[11] Facchini, B., Maiuolo, F., Tarchi, L., and Coutadin, D., 2012. "Experimental investigation on the effects of a large recirculating area on the performance of an effusion cooled combustor liner". *Journal of Engineering for Gas Turbines and Power,* **134**.

[12] Ekkad, S. V., Zapata, D., and Han, J. C., 1997. "Film effectiveness over a flat surface with air and co2 injection through compound angle holes using a transient liquid crystal image method". *ASME Journal of Turbomachinery,* **119**, pp. 587–593.

[13] Ekkad, S. V., Zapata, D., and Han, J. C., 1997. "Heat transfer coefficient over a flat surface with air and co2 injection through compound angle holes using a transient liquid crystal image method". *ASME Journal of Turbomachinery,* **119**, pp. 580–585.

[14] Lin, Y., Song, B., Li, B., Liu, G., and Wu, Z., 2003. "Investigation of film cooling effectiveness of full-coverage inclined multihole walls with different hole arrangements". *ASME Turbo Expo*(GT2003-38881).

[15] Lin, Y., Song, B., Li, B., and Liu, G., 2006. "Investigation of film cooling effectiveness of full-coverage inclined multihole walls with different hole arrangements". *ASME Journal of Heat Transfer,* **128**, pp. 580–585.

[16] Andreini, A., Ceccherini, A., Facchini, B., and Coutadin, D., 2010. "Combined effect of slot injection, effusion array and dilution hole on the heat transfer coefficient of a real combustor liner - part 2 numerical analysis". *ASME Turbo Expo*(GT2010-22937).

[17] Roach, P. E., 1987. "The generation of nearly isotropic turbulence by means of grids". *Heat and Fluid Flow,* **8(2)**, pp. 83–92.

[18] Chan, T. L., Ashforth-Frost, S., and Jambunathan, K., 2001. "Calibrating for viewing angle effect during heat transfer measurements on a curved surface". *International Journal of Heat and Mass Transfer,* **44**, pp. 2209–2223.

[19] L'Ecuyer, M. R., and Soechting, F. O., 1985. "A model for correlating flat plate film cooling effectiveness for rows of round holes". In *AGARD Heat Transfer and Cooling in Gas Turbines 12p (SEE N86-29823 21-07)*. Sept.

[20] ASME, 1985. "Measurement uncertainty". In *Instrument and Apparatus*, Vol. ANSI/ASME PTC 19.1-1985 of *Performance Test Code*. ASME.

[21] Kline, S. J., and McClintock, F. A., 1953. "Describing uncertainties in single sample experiments". *Mechanical Engineering,* **75**, Jen, pp. 3–8.

[22] Sen, B., Schmidt, D. L., and Bogard, D. G., 1996. "Film cooling with compound angle holes: Heat transfer". *ASME Journal of Turbomachinery,* **118**, pp. 800–806.

[23] Gritsch, M., Schulz, A., and Wittig, S., 2000. "Film-cooling holes with expanded exits: near-hole heat transfer coefficients". *International Journal of Heat and Fluid Flow,* **21**, pp. 146–155.

[24] Christophel, J. R., Thole, K. A., and Cunha, F. J., 2005. "Cooling the tip of a turbine blade using pressure side holes-part ii: Heat transfer measurements". *ASME Turbo Expo*(2004-GT-53254).

[25] Piggush, J. D., and Simon, T. W., 2007. "Measurements of net change in heat flux as a result of leakage and steps on the contoured endwall of a gas turbine first stage nozzle". *Applied Thermal Engineering,* **27**, pp. 722–730.

[26] Lefebvre, A. H., 1998. *Gas Turbine Combustion*. Taylor & Francis.

[27] Andreini, A., Carcasci, C., Ceccherini, A., Facchini, B., Surace, M., Coutandin, D., Gori, S., and Peschiulli, A., 2007. "Combustor liner temperature prediction: a preliminary tool development and its application on effusion cooling systems". *First CEAS European Air and Space Conference Century Perspectives*(Paper n.026).

[28] Andreini, A., Ceccherini, A., Facchini, B., Turrini, F., and Vitale, I., 2009. "Assesment of a set of numerical tools for the design of aeroengines combustors: study of a tubular test rig". *ASME Turbo Expo*(GT2009-59539).